Title
Inhibition by anandamide of gap junctions and intercellular calcium signalling in striatal astrocytes

Journal
Nature, 376(6541)

ISSN
0028-0836

Authors
Venance, Laurent
Piomelli, Daniele
Glowinski, Jacques
et al.

Publication Date
1995-08-01

DOI
10.1038/376590a0

simply looking at possible or impossible objects, as opposed to a condition in which non-object stimuli are presented, produces differential blood flow increases for possible and impossible objects. A study using additional controls is necessary to determine how the blood flow changes reported here are related to those involved in passive perception of possible and impossible objects.

Additional significant blood flow changes will be described in a subsequent report. For instance, for both possible and impossible objects, the new-object decision, old-object decision, new recognition and old recognition minus no-decision baseline comparisons all revealed increases in the vicinity of dorsolateral prefrontal cortex (Brodmann areas 10, 44–46), which could be involved in the executive operations associated with making a decision.

Our study provides direct neuroanatomical evidence from the normal human brain that inferior temporal and fusiform gyri are selectively involved in computing global representations of structurally coherent three-dimensional objects, and extends our knowledge of the neural systems involved in episodic memory for visual objects. □

Received 28 October 1994; accepted 28 June 1995.

1. Miyashita, Y. *A. Rev. Neurosci.* **16,** 245–269 (1993).
2. Schacter, D. L., Cooper, L. A., Tharan, M. & Rubens, A. B. *J. cogn. Neurosci.* **3,** 118–131 (1991).
3. Tanaka, K. *Science* **262,** 685–688 (1993).
4. Schacter, D. L., Cooper, L. A. & Delaney, S. M. *J. exp. Psychol.* **119,** 5–24 (1990).
5. Collins, D. L., Neelin, P., Peters, T. M. & Evans, A. C. *J. comput. assist. Tomogr.* **18,** 192–204 (1994).
6. Friston, K. J. *et al. J. cerebr. Blood Flow Metab.* **10,** 458–466 (1991).
7. Talairach, J. & Tournoux, P. *Co-planar Stereotaxic Atlas of the Human Brain* (Thieme Medical, New York, 1988).
8. Mintun, M. A. & Lee, K. S. *J. nucl. Med.* **31,** 816 (1991).
9. Gross, C. G. *Phil. Trans. R. Soc.* B**335,** 245–246 (1992).
10. Cooper, L. A., Schacter, D. L., Ballesteros, S. & Moore, C. *J. exp. Psychol., Learn. Mem. Cogn.* **18,** 43–57 (1992).
11. Kosslyn, S. M. *et al. Brain* (in the press).
12. Sergent, J., Ohta, S. & MacDonald, B. *Brain* **115,** 15–36 (1992).
13. Allison, T. *et al. J. Neurophysiol.* **71,** 821–825 (1994).
14. Damasio, A. R., Damasio, H. & VanHoesen, G. W. *Neurology* **32,** 331–341 (1982).
15. Haxby, J. V. *et al. J. Neurosci.* **14,** 6336–6353 (1994).
16. Gray, J. A. *The Neuropsychology of Anxiety* (Oxford Univ. Press, 1982).
17. Stern, C. *et al. Soc. Neurosci. Abstr.* **20,** 530 (1994).
18. Tulving, E. *et al. NeuroReport* **5,** 2525–2528 (1994).
19. Vinograda, O. S. *The Hippocampus* Vol. 2 (eds Isaacson, R. L. & Pribram, K. H.) (Plenum, New York, 1978).
20. Robinson, D. L. & Petersen, S. E. *Trends Neurosci.* **15,** 127–132 (1992).
21. Frackowiak, R. S. J. *Trends Neurosci.* **17,** 109–115 (1994).
22. Grasby, P. M. *et al. Neurosci. Lett.* **163,** 185–188 (1993).
23. Jones-Gotman, M. *et al. Soc. Neurosci. Abstr.* **19,** 1002 (1993).
24. Squire, L. R. *et al. Proc. natn. Acad. Sci. U.S.A.* **89,** 1837–1841 (1992).
25. Shallice, T. *et al. Nature* **368,** 633–635 (1994).
26. Tulving, E. *et al. Proc. natn. Acad. Sci. U.S.A.* **91,** 2012–2015 (1994).
27. Buckner, R. *et al. J. Neurosci.* **15,** 12–29 (1995).
28. Buckner, R. & Tulving, E. *Handbook of Neuropsychology* (eds Boller, F. & Grafman, J.) 439–466 (Elsevier, Amsterdam, 1995).
29. Schacter, D. L. & Cooper, L. A. *J. exp. Psychol., Learn. Mem. Cogn.* **19,** 995–1009 (1993).

ACKNOWLEDGEMENTS. We thank D. Bandy, N. Blocher, A. Evans, M. Mintun, K. Nelson and K. Zemanick for their assistance. This work was supported by grants from the McDonnell-Pew Program in Cognitive Neuroscience, the Robert S. Flinn Foundation, and the NIMH.

Inhibition by anandamide of gap junctions and intercellular calcium signalling in striatal astrocytes

Laurent Venance*, Daniele Piomelli†, Jacques Glowinski* & Christian Giaume*‡

* INSERM U114, Collège de France, 11 Place Marcelin Berthelot, 75231 Paris Cedex 05, France
† The Neurosciences Institute, 3377 North Torrey Pines Court, La Jolla, California 90237, USA

ANANDAMIDE, an endogenous arachidonic acid derivative that is released from neurons and activates cannabinoid receptors[1], may act as a transcellular cannabimimetic messenger in the central nervous system[2–4]. The biological actions of anandamide and the identity of its target cells are, however, still poorly documented[5]. Here we show that anandamide is a potent inhibitor of gap-junction conductance and dye permeability in striatal astrocytes. This inhibitory effect is specific for anandamide as compared to co-released congeners[4] or structural analogues, is sensitive to pertussis toxin and to protein-alkylating agents, and is neither mimicked by cannabinoid-receptor agonists nor prevented by a cannabinoid-receptor antagonist. Glutamate released from neurons evokes calcium waves in astrocytes[6] that propagate via gap junctions[7–9], and may, in turn, activate neurons distant from their initiation sites in astrocytes[10–12]. We find that anandamide blocks the propagation of astrocyte calcium waves generated by either mechanical stimulation or local glutamate application. Thus, by regulating gap-junction permeability, anandamide may control intercellular communication in astrocytes and therefore neuron–glial interactions.

The conductance of gap junctions (GJ) was monitored in pairs of cultured striatal astrocytes from embryonic mice by using the double whole-cell recording (DWCR) method[13] (Fig. 1*Aa*, *b*). The junctional conductance, which was 14.4 ± 2.7 nS (mean ± s.e.m.; $n = 26$) in the control, was reduced to 1.1 ± 1.2 nS ($n = 14$, in which 8 pairs were completely uncoupled) by 5 μM anandamide, but not by the cannabinoid agonist CP55940 (1 μM) (20.5 ± 5.3 nS; $n = 6$) (Fig. 1*B*). This inhibitory effect of anandamide on GJ permeability was confirmed by using the scrape-loading dye-transfer technique[14]. The intercellular diffusion of Lucifer yellow was significantly decreased and even greatly inhibited when the cells were incubated for 10 min with anandamide (1 μM and 5 μM, respectively) (Fig. 1*Ca–c*, *D*). The inhibition evoked by anandamide (5 μM) was reversible, and comparable to that evoked by the uncoupling agent 18α-glycyrrhetinic acid[15] (10 μM) (Fig. 1*D*), being already apparent after 2 min exposure (data not shown).

In contrast to anandamide, two synthetic cannabinoid-receptor agonists, Win-55212-2 (5 μM) and CP55940 (1 μM), had no effect on GJ permeability (Fig. 1*D*), although at the same concentrations these two compounds, as anandamide, inhibited the isoprenaline(1 μM)-induced production of cyclic AMP in striatal astrocytes (S. Sagan, unpublished results). Moreover, the antagonist at CB1-type cannabinoid receptors[16], SR141716A (0.5 μM; 10 min pretreatment), did not reduce the anandamide response (Fig. 1*D*). Therefore, anandamide seems to modulate GJ permeability in striatal astrocytes through a mechanism distinct from central cannabinoid-receptor activation. When cells were pretreated in the presence of the phosphodiesterase inhibitor IBMX (1 mM) with agents known to increase cAMP concentration (such as isoprenaline or forskolin, at 10 μM for 10 min), the effectiveness of anandamide on GJ permeability was not altered, suggesting that a reduction of cAMP level is not involved in this process. In addition, neither the protein-kinase inhibitors H7(0.1 mM, 30 min) or staurosporine (1 μM, 30 min), which have a large range of action, nor the phosphatase inhibitor okadaic acid (0.1 μM, 40 min) prevented GJ uncoupling induced by anandamide (5 μM, 10 min).

The chemical structure of anandamide (*N*-arachidonoyl ethanolamine) includes the polyunsaturated fatty acyl moiety of arachidonic acid (AA), which inhibits GJ permeability in astrocytes[17]. However, several observations suggested that anandamide does not act directly on striatal astrocyte GJ by mimicking the uncoupling effect of exogenous application of AA. First, anandamide was ~10 times more potent than AA in uncoupling striatal astrocytes (Fig. 1*D*). Second, pertussis toxin

‡ To whom correspondence should be addressed.

(PTX), which ADP-ribosylates and inhibits Gi/oα-proteins, markedly reduced the GJ uncoupling evoked by anandamide (5 μM), but not that produced by AA (50 μM) (Fig. 1*Cd*, *e*, *E*). This lack of effect of PTX on AA-induced inhibition of GJ permeability was not due to the use of a saturating concentration of AA, because at 10 μM, when partial uncoupling (40 ± 4% of control, $n = 3$) occurred, PTX treatment had no significant effect (47 ± 10%, $n = 3$). Furthermore, *N*-ethylmaleimide, an alkylating agent that inhibits G proteins[18], and the histidine alkylating agent 4-bromophenacyl bromide each prevented inhibition by anandamide (5 μM) but not by AA (50 μM) (Fig. 1*E*).

The selectivity of anandamide was supported further by experiments with structural analogues. We synthesized four anandamide analogues in which the *N*-arachidonoyl moiety was replaced with moieties of equal chain length (20 carbon atoms) but having a decreasing number of double bonds (3, 2, 1 or 0 instead of 4). At a concentration (5 μM) at which anandamide induced a potent response on GJ permeability in striatal astrocytes, none of these analogues had any significant effect (Fig. 2*a*, and data not shown). Together with anandamide, a family of five *N*-acyl-ethanolamines are released from stimulated striatal neurons[4]. These congeners were not effective when used at 5 μM (Fig. 2*a* and data not shown), but two of them, *N*-oleoyl-

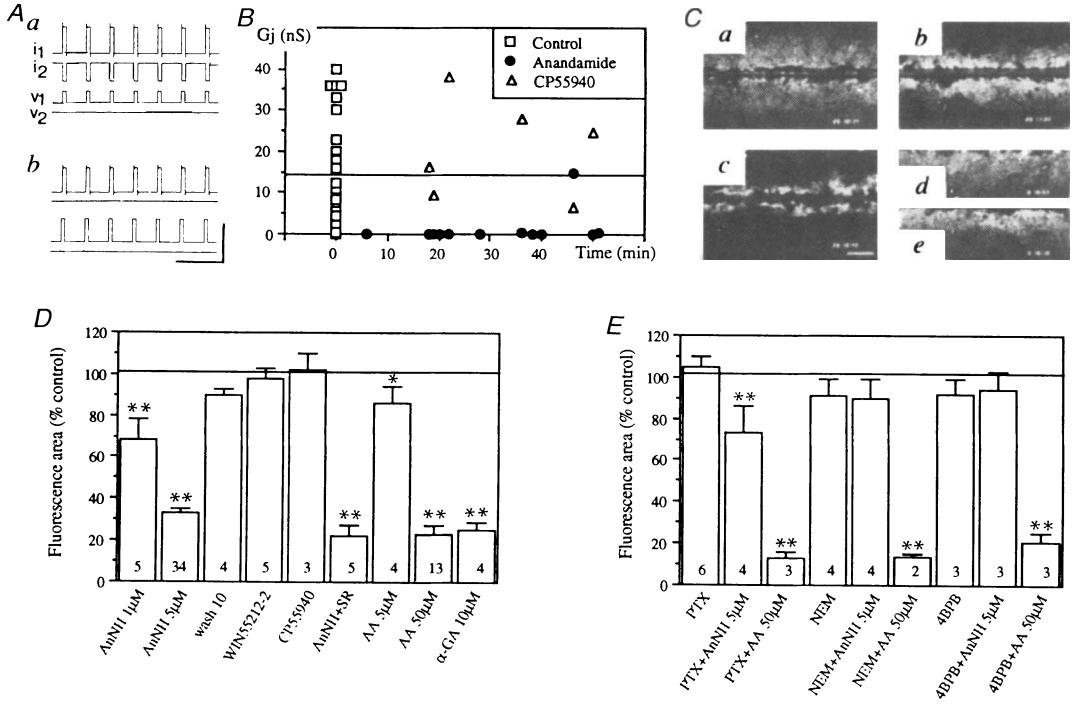

FIG. 1 Inhibition by anandamide of GJ conductance and dye permeability in primary cultures of striatal astrocytes from mouse embryos. *A*, Currents recorded from pairs of astrocytes using the DWCR technique[13]: control junctional current (i_2) was monitored when a voltage difference ($V_1 - V_2$) was applied between the two cells from a −70 mV holding potential (*a*). In the presence of 5 μM anandamide (*b*), no junctional current was detected in another pair of cells from the same dish (calibrations: 2, 0.5 nA and 2, 0.2 nA, for i_1 and i_2 in *a* and *b* respectively, 200 mV for V_1 and V_2, 2 s). *B*, Effects of anandamide (5 μM) and CP55940 (1 μM) on junctional conductance (G_j, ordinate). G_j was measured 1–2 min after establishment of the DWCR by applying transjunctional voltage pulses, ranging from +50 mV to +100 mV, and then plotted as a function of time (abscissa). One or two G_j values were measured in each dish; all these control points were arbitrarily plotted at time 0 when either anandamide or CP55940 were added to the bath. The horizontal line represents the averaged value (14.4 nS) of the controls. *C*, Fluorescence photomicrographs of scrape-loading experiments: *a*, control, 10 min after loading, Lucifer yellow (LY) diffused widely throughout the confluent layer of astrocytes; *b*, 1 μM anandamide significantly reduced dye diffusion; *c*, 5 μM anandamide blocked dye spread; *d*, PTX treatment had no significant effect (1 μg ml^{-1}, 24 h); *e*, the inhibitory effect of 5 μM anandamide was reduced by PTX treatment (*d* and *e* represent half of photomicrographs; calibration bar, 250 μm). *D*, *E*, averaged values (mean ± s.e.m.) of the surface area stained with Lucifer yellow, measured under various conditions and expressed as percentage of the internal controls. Drugs were applied for 10 min before scrape-loading and used at the concentrations indicated in the text. Pretreatments with NEM (50 μM) and 4BPB (10 μM) were made 10 and 30 min before anandamide or AA application, respectively. The number of independent experiments performed are indicated inside the columns. Statistical analysis: one-way ANOVA followed by *post hoc* Dunnett's multiple comparison test. Significance was established at $P < 0.05$ (*) and $P < 0.01$ (**). Horizontal line indicates the level of fluorescence area determined in control conditions. Abbreviations: AnNH, anandamide; PTX, pertussis toxin; α-GA, 18α-glycyrrhetinic acid; NEM, *N*-ethylmaleimide; 4BPB, 4-bromophenacyl bromide.

METHODS. Primary cultures of astrocytes were prepared as described[17,26]. Selected brain structures were removed from 16-day-old Swiss mouse embryos. The culture medium, a mixture of EM medium and F12 nutrient (1:1) supplemented with 10% NU serum, was changed weekly (serum was omitted 4 days before experiments). Experiments were done at room temperature on 18–24-day-old cultures, in which up to 95% of the cells were identified as astrocytes by using an antibody against the glial fibrillary acidic protein (GFAP). External solution contained (in mM): NaCl 140, KCl 5.5, $CaCl_2$ 1.8, $MgCl_2$ 1, glucose 25 and HEPES 10, pH 7.3. Junctional conductance was monitored using the DWCR technique[13] performed on pairs of astrocytes prepared as described[26], with a recording pipette solution containing (in mM): KCl 140, $MgCl_2$ 1, EGTA 5 and HEPES 10, pH 7.3. GJ permeability was determined using the scrape-loading technique[14]. Cell loading was achieved with a blade in the external solution (without calcium) containing 0.1% LY; 1 min later, cells were washed several times with the standard external solution. When a cocktail of LY (M_r 457) and rhodamine–dextran (M_r 10,000) was used, the localization of the second dye, to which GJs are impermeable, was restricted to the initially loaded cells, whereas LY diffused to neighbours (*C*, *a*). GJ permeability was assessed 9 min after scraping by taking photomicrographs of five adjacent hemifields. Analysis was carried out with an image analyser system (Imstar software), measuring the fluorescence area from digitized images[17]. Quantification was then achieved by expressing the measured area as a percentage of its internal control. Applications of vehicles (methanol, 1/2,000; ethanol 1/2,000: dimethylsulphoxide, 1/20,000) alone had no effect on GJ permeability.

TABLE 1 Effects of different agents on the propagation of calcium waves in striatal astrocytes

	Experimental conditions	Number of cells in the field (no. of experiments)	Number of responding cells (%)	Ratio (F405/F480) of stimulated cell (no. of cells)	Ratio (F405/F480) of the cells of the first row (no. of cells)
Mechanical stimulation	Control	34 ± 1 (25)	28 ± 1 (82%)	1.17 ± 0.04 (25)	0.76 ± 0.07 (137)
	Anandamide 0.01 μM	33 ± 1 (14)	29 ± 1.4 (88%)	1.17 ± 0.03 (14)	0.71 ± 0.03 (96)
	0.1 μM	36 ± 1 (13)	30 ± 1 (83%)	1.24 ± 0.08 (13)	0.86 ± 0.03 (92)
	0.5 μM	30 ± 2 (4)	11 ± 1 (37%)	1.03 ± 0.14 (4)	0.17 ± 0.02 (11)
	1 μM	30 ± 4 (4)	5 ± 1 (15%)	0.96 ± 0.06 (4)	0.16 ± 0.01 (17)
	5 μM	32 ± 2 (15)	4 ± 0.8 (13%)	1.03 ± 0.05 (15)	0.27 ± 0.03 (35)
	Win 55212-2 5 μM	34 ± 2 (3)	25 ± 1.8 (74%)	1.39 ± 0.02 (3)	0.58 ± 0.06 (19)
	C18:1 30 μM	31 ± 2 (5)	24 ± 1 (77%)	1.09 ± 0.11 (5)	0.56 ± 0.06 (30)
	Arachidonic acid 10 μM	35 ± 2 (15)	4 ± 1 (11%)	1.04 ± 0.05 (15)	0.25 ± 0.04 (23)
	18α-glycyrrhetinic acid 10 μM	30 ± 3 (4)	2 ± 1 (7%)	1.06 ± 0.12 (4)	0.16 ± 0.08 (4)
Local application of glutamate (100 μM)	Control	30 ± 1 (11)	11 ± 0.8 (37%)	0.43 ± 0.04 (11)	0.29 ± 0.02 (36)
	Anandamide 5 μM	29 ± 1 (20)	2 ± 0.4 (6%)	0.34 ± 0.03 (20)	0.13 ± 0.02 (21)

Averaged values given in the second column represent the number of cells in which a rise in $[Ca^{2+}]_i$ was recorded (responding cells); percentages are expressed versus the number of total cells in the microscopic field. Velocity of intercellular calcium waves, generated either by mechanical stimulation or local glutamate application, were calculated from control experiments and were 17 ± 1 μm s^{-1} and 15 ± 1 μm s^{-1}, respectively. Results are expressed as mean ± s.e.m.

ethanolamine and *N*-γ-linolenoyl-ethanolamine, had a significant, albeit partial, effect at 30 μM and 10 μM, respectively; these concentrations take into account their ratio of co-release with anandamide[4] (Fig. 2*a*).

We then determined whether the ability of anandamide to inhibit GJ dye permeability was different in astrocyte cultures prepared from various brain structures. In contrast to the marked uncoupling observed in striatal astrocytes, anandamide (5 μM) only partially affected GJ permeability in astrocytes from other brain structures. No such regional specificity was observed with AA used at concentrations that produce either partial (10 μM) or complete (50 μM) uncoupling in striatal astrocytes (Fig. 2*b*).

In astrocytes, GJs provide a pathway for the propagation of intercellular calcium waves[7–9], which in turn may be important in astrocyte–neuron interactions[10–12,19]. Striatal astrocytes were loaded with Indo1-AM to determine the effect of anandamide on calcium waves. Mechanical stimulation of individual astrocytes[7] induced a rapid rise in intracellular free calcium level ($[Ca^{2+}]_i$), which spread to distant astrocytes (Fig. 3*a*). Anandamide (5 μM) blocked these calcium waves as in this case only direct neighbours of the stimulated cell showed slight rises in $[Ca^{2+}]_i$ (Fig. 3*b* and Table 1). Such an effect was already detected with a concentration of anandamide as low as 0.5 μM (Table 1), similar to that required to inhibit the isoprenaline-induced production of cAMP in striatal astrocytes (S. Sagan, unpublished results) and to obtain half-maximal activation of cannabinoid receptors in other intact cells[20]. Owing to the rapid astrocytic uptake and hydrolic degradation of anandamide[4,21], the effective concentration of this compound may have even been lower than 0.5 μM. Although lower concentrations of anandamide (0.1 and 0.01 μM) had no effect, calcium waves were also blocked by AA (10 μM) and 18α-glycyrrhetinic acid (10 μM) but not by *N*-oleoyl-ethanolamine (30 μM) or Win 55212-2 (5 μM) (Table 1). Calcium waves were also elicited by applying the excitatory neurotransmitter, glutamate, onto individual astrocytes with a pressure-operated micropipette (Fig. 3*c*). These waves, which propagated typically along circuitous

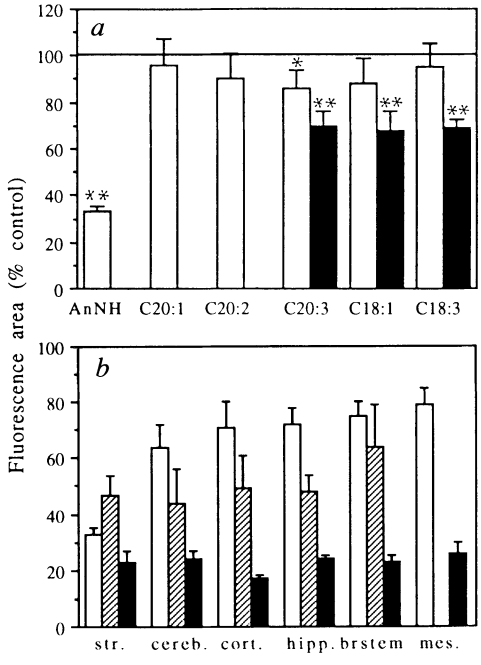

FIG. 2 Structural and regional specificity of anandamide-induced inhibition of astrocyte GJ permeability. *A*, Effects of anandamide (*N*-arachidonoyl-ethanolamine, AnNH), *N*-eicosamonoenoyl-ethanolamine (C20:1), *N*-eicosadienoyl-ethanolamine (C20:2), *N*-eicosatrienoyl-ethanolamine (C20:3), *N*-oleoyl-ethanolamine (C18:1) and *N*-γ-linolenoyl-ethanolamine (C18:3) on GJ permeability in striatal astrocytes. Concentrations used were 5 μM (empty columns) and 10 μM (for C18:3 and C20:3) or 30 μM (for C18:1) (filled columns). *b*, Effects of 5 μM anandamide (empty columns), 10 μM (hatched columns) and 50 μM AA (filled columns) on GJ permeability of astrocyte cultured from striatum (str.), cerebellum (cereb.), cortex (cort.), hippocampus (hipp.), brainstem (br. stem), and mesencephalon (mes.). Drugs were applied for 10 min before scrape-loading. The number of independent experiments shown in *a* and *b* varied from 3 to 34. Statistical analysis: in *a*, significance was established at $P < 0.01$ (*) and $P < 0.0001$ (**) with Student's *t*-test; in *b*, using one-way ANOVA followed by *post hoc* Student–Newman–Keuls's multiple comparisons, test significance was established at $P < 0.001$ for anandamide in striatum versus other structures, but no significance was found for all structures with AA at 10 μM and 50 μM ($P > 0.05$).

METHODS. Primary cultures of astrocytes were prepared and used as described in Fig. 1 legend, except for the mesencephalon and the cerebellum, which were prepared from 14-day-old embryos and newborn animals, respectively. Anandamide and its analogues were synthesized[4] and purified by high-performance liquid chromatography as described[2]. All products were kept in methanol (10 mM) at −80 °C, and diluted in standard ionic solutions immediately before the experiments.

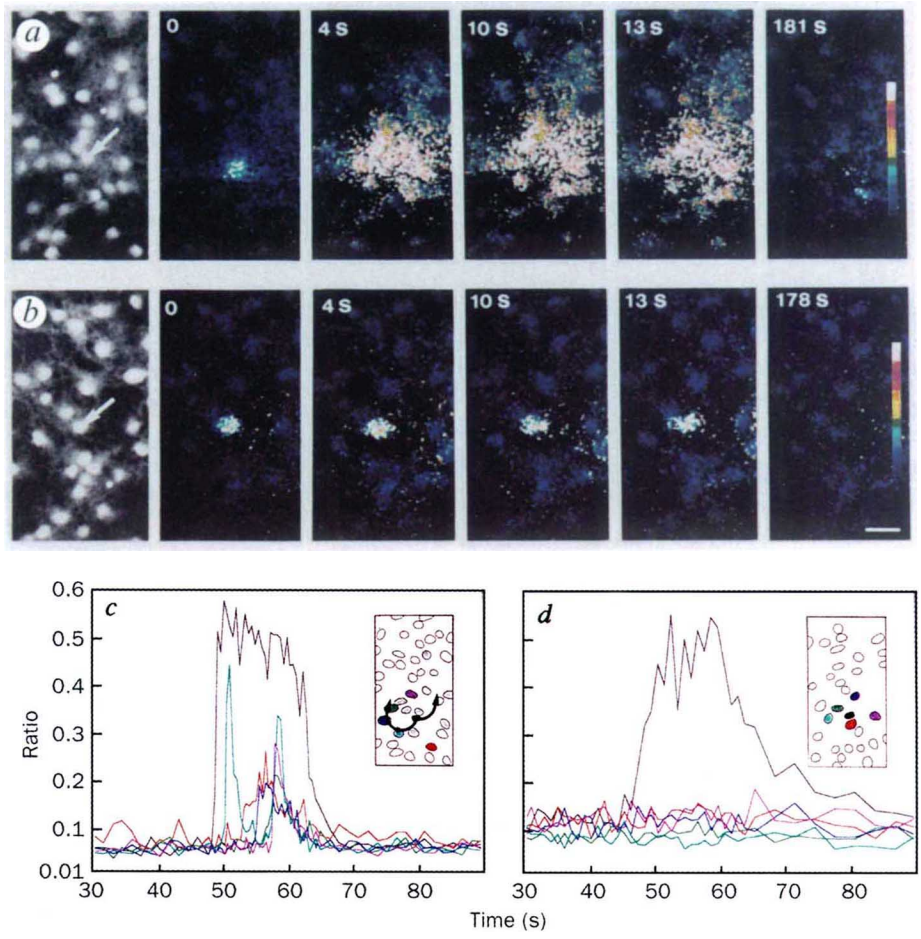

FIG. 3 Blockage by anandamide of propagation of calcium waves in primary cultures of rat striatal astrocytes. Changes in $[Ca^{2+}]_i$ were monitored by calcium imaging. Mechanical stimulation of individual astrocytes (arrows), carried out in the absence (*a*) or presence (*b*) of anandamide (5 μM). Left, fluorescent images ($\lambda_{emission} = 480$ nm) of two fields of astrocytes loaded with Indo1-AM; right, sequential pseudocolour representations of $[Ca^{2+}]_i$ expressed as the ratio of indol-AM emissions at 405 and 480 nm due to excitation at 355 nm. Calcium increase initiated in the stimulated cell rapidly propagated in all directions to most cells present in the microscopic field ($t = 13$ s). In the control experiment (*a*) the averaged calcium basal level of the cells in the investigated field was 0.10 ± 0.01 ($n = 37$ cells) before mechanical stimulation, and the peak of $[Ca^{2+}]_i$ changes following mechanical stimulation varied from 0.18 to 1.46 ($n = 34$ cells). In the presence of anandamide (*b*), basal calcium was 0.11 ± 0.01 nM ($n = 27$ cells) and the mean peak of $[Ca^{2+}]_i$ change induced in the stimulated cell and the adjacent cells varied from 0.06 to 1.22 nM ($n = 6$ cells). Pseudocolour scale bars refer to ratios from 0.01 to 1.50, which corresponded to estimated $[Ca^{2+}]_i$ values of 10 nM to 2,000 nM, respectively (calibration bar, 25 μm). Stimulation of individual astrocytes by pressure application of glutamate (100 μM, ~276 kPa, 20 ms) either in the absence (*c*) or presence (*d*) of anandamide (5 μM). Insets: schematic drawings of astrocyte cell bodies in the inspected microscopic fields. Black, astrocytes receiving the glutamate puffs; colour, cells in which fluorescence was plotted; grey, additional responding cells. Arrows indicate the paths of two separate calcium waves evoked by glutamate application.

METHODS. Striatal astrocytes from 18-day-old rat embryos were maintained in culture as described for Fig. 1, except that they were plated on glass coverslides coated with poly-L-ornithine and laminin[27]. Intracellular calcium levels were measured by dual emission microfluorimetry using the fluorescent dye Indo1-AM[27]. $[Ca^{2+}]_i$ was calculated from the fluorescence ratio (measured at 400–410 nm and 470–480 nm) according to Grynkiewicz's equation[28], with a K_d of 250 nM for the Indo1-AM. Images were acquired every 1–3 s with an image-processing system (Hamamatsu Argus 50) and an inverted microscope (Nikon Diaphot) and then recorded on an optical disk memory (Laser Magnetic Storage International Company). Experiments were carried out at room temperature in a solution containing (in mM); NaCl 145, KCl 5.5, $CaCl_2$ 1.1, $MgCl_2$ 0.9, glucose 12 and HEPES 20, pH 7.3.

paths[8], were also blocked by anandamide (5 μM) (Fig. 3*d* and Table 1).

Our results show that anandamide inhibits GJ conductance and dye permeability, and blocks GJ-mediated propagation of calcium signalling in striatal astrocytes. Because of its brain-structure specificity, structural selectivity, sensitivity to G-protein inhibitors and to mild protein-alkylating agents, the anandamide GJ inhibition could be mediated through a specific receptor. Such a putative receptor may be distinct from any of the two known cannabinoid receptor subtypes[5], as suggested by the lack of effect of either cannabinoid-receptor agonists or CB-1 antagonist. Further supporting this possibility, recent studies have indicated that anandamide, a partial agonist at cannabinoid receptors[18], may exert several pharmacological actions distinct from those of plant-derived or synthetic cannabinoid drugs[22].

Glutamate released from nerve terminals evokes calcium waves in adjacent astrocytes[7]. In turn, these waves propagate through the astrocyte network[23] and trigger responses in neurons embedded within it[10–12]. Our findings suggest that this long-range signalling loop between neurons and astrocytes may be turned off by anandamide. Thus anandamide, a transcellular messenger produced and released from neurons but not from astrocytes[2–4], may modulate synaptic function not only locally by controlling neuronal transmitter release through the regulation of calcium channels[18], but also distally by preventing the recruitment of subpopulations of astrocytes and the subsequent activation of contacting groups of neurons. It remains to be determined whether such a distal action of anandamide occurs as well *in vivo* in the striatum, where its astrocyte-uncoupling effect is most prominent and the existence of functional compartments of neuronal groups receiving somatotopic glutamatergic cortical afferents has been demonstrated[24,25]. □

Received 19 April; accepted 26 June 1995.

1. Devane, W. A. *et al. Science* **258,** 1946–1949 (1992).
2. Krusza, K. K. & Gross, R. W. *J. biol. Chem.* **269,** 14345–14348 (1994).
3. Devane, W. A. & Axelrod, J. *Proc. natn. Acad. Sci. U.S.A.* **91,** 6698–6701 (1994).
4. Di Marzo, V. *et al. Nature* **372,** 686–691 (1994).
5. Devane, W. A. *Trends pharmacol. Sci.* **15,** 40–41 (1994).
6. Dani, J. W., Chernjavsky, A. & Smith, S. J. *Neuron* **8,** 429–440 (1992).
7. Charles, A. C. *et al. J. Cell Biol.* **118,** 195–201 (1992).
8. Finkbeiner, S. M. *Neuron* **8,** 1101–1108 (1992).
9. Enkvist, M. O. K. & McCarthy, K. D. *J. Neurochem.* **59,** 519–526 (1992).
10. Nedergaard, M. *Science* **263,** 1768–1771 (1994).
11. Parpura, V. *et al. Nature* **369,** 744–747 (1994).
12. Charles, A. C. *Devl Neurosci.* **16,** 196–206 (1994).
13. Neyton, J. & Trautmann, A. *Nature* **317,** 331–335 (1985).
14. El-Fouly, M. H., Trosko, J. E. & Chang, C. *Expl Cell Res* **168,** 422–430 (1987).
15. Davidson, J. S., Baumgarten, I. M. & Harley, E. H. *Biochem. biophys. Res. Commun.* **134,** 29–36 (1986).
16. Rinaldi-Carmona, M. *et al. FEBS Lett.* **350,** 240–244 (1994).
17. Giaume, C., Marin, P., Cordier, J., Glowinski, J. & Prémont, J. *Proc. natn. Acad. Sci. U.S.A.* **88,** 5577–5581 (1991).
18. Mackie, K., Devane, W. A. & Hille, B. *Molec. Pharmac.* **44,** 498–503 (1993).
19. Smith, S. *Curr. Biol.* **4,** 807–811 (1994).
20. Felder, C. C. *et al. Proc. natn. Acad. Sci. U.S.A.* **90,** 7656–7660 (1993).

21. Desarnaud, F., Cadas, H. & Piomelli, D. *J. biol. Chem.* **270,** 6030–6035 (1995).
22. Smith, P. B. *et al. J. Pharmac. Exp. Ther.* **270,** 219–227 (1994).
23. Cornell-Bell, A., Finkbeiner, S. M., Cooper, M. S. & Smith, S. J. *Science* **247,** 470–473 (1990).
24. Gerfen, C. R. *Trends Neurosci.* **15,** 133–139 (1992).
25. Graybiel, A. M., Aosaki, T., Flaherty, A. W. & Kimura, M. *Science* **265,** 1826–1831 (1994).
26. Giaume, C. *et al. Neuron* **6,** 133–143 (1991).
27. Murphy, N. P., Cordier, J., Glowinski, J. & Prémont, J. *Eur. J. Neurosci.* **6,** 854–860 (1994).
28. Grynkiewicz, G., Poeni, M. & Tsien, R. *J. biol. Chem.* **260,** 3440–3450 (1985).

ACKNOWLEDGEMENTS. We thank J. A. Girault, J. Prémont, S. Sagan, N. Stella, A. Trautmann and R. Williams for comments on the manuscript, and G. Lefur of Sanofi Recherche for the cannabinoid receptor antagonist SR14716A.

An IL-12-based vaccination method for preventing fibrosis induced by schistosome infection

Thomas A. Wynn*, Allen W. Cheever†, Dragana Jankovic*, Robert W. Poindexter†, Pat Caspar*, Fred A. Lewis‡ & Alan Sher*

* Immunobiology Section and † Host–Parasite Relations Section, Laboratory of Parasitic Diseases, National Institute of Allergy and Infectious Diseases, National Institutes of Health, Bethesda, Maryland 20892, USA
‡ The Biomedical Research Institute, Rockville, Maryland 20852, USA

THE harmful fibrosis which often occurs in the context of infectious disease involves the excessive deposition of connective tissue matrix, particularly collagen, and is mostly resistant to pharmacological and immunological intervention[1]. In schistosomiasis, fibrosis is associated with the granulomatous response to parasite eggs trapped in the liver[2]. We have previously shown that interleukin (IL)-12 administered peritoneally with eggs prevents subsequent pulmonary granuloma formation on intravenous challenge with eggs[3]. Here we show that sensitization with eggs plus IL-12 partly inhibits granuloma formation and dramatically reduces the tissue fibrosis induced by natural infection with *Schistosoma mansoni* worms. These results are an example of a vaccine against parasites which acts by preventing pathology rather than infection. IL-12 is known to favour the priming of Th1 rather than Th2 cells, and the effects on fibrosis are accompanied by replacement of the Th2-dominated pattern of cytokine expression characteristic of *S. mansoni* infection with one dominated by Th1 cytokines. Elevated Th2 cytokine expression and fibrosis are common manifestations of a wide variety of infectious diseases and atopic disorders which might be ameliorated by vaccination with antigen and IL-12.

Mice of the C57BL/6 strain were inoculated with *S. mansoni* eggs, either with or without IL-12, and then exposed to percutaneous infection by *S. mansoni* larvae (cercariae). Egg/IL-12 sensitization did not significantly reduce the number of worms or eggs recovered early in infection at either 8 or 12 weeks (Table 1). Nevertheless, sensitization with eggs/IL-12 had pronounced effects on host pathology. Granulomas were evident in the egg/IL-12 group, but the lesions were significantly smaller and contained fewer eosinophils than those observed in infected unsensitized mice (Table 1). Sensitization with eggs alone resulted in a smaller decrease in granuloma size, comparable to that seen in previous studies[4]. The most striking effect of egg/IL-12 sensitization was the inhibition of egg-induced hepatic fibrosis, as illustrated by tissue sections stained for collagen (Fig. 1). Compared with control mice at 8 and 12 weeks, mice sensitized with egg/IL-12 showed reductions in hepatic hydroxyproline (a chemical measure of collagen content) of 58.0% and 72.2%, respectively, and reductions of 19.5% and 35.5% were observed in the egg/saline group (Table 1). When levels of messenger RNA for type I and type III collagen are compared (Fig. 2), the differences between the three groups of mice are greatest at 8 weeks, during the initial phase of synthesis of these proteins. Sensitization with eggs/IL-12 caused a nearly tenfold reduction in the levels of induced expression of liver type I and type III mRNAs relative to that seen in unsensitized mice. A 2.5-fold and 4-fold reduction was seen in the same mRNAs in the egg/saline group. The observed sensitization-dependent decrease in tissue pathology was not accompanied by increases in necrosis within granulomas.

Previous studies have demonstrated an influence of Th2 cytokines on hepatic granuloma formation and fibrosis[5,6], and a suppressive effect of IL-12 on egg-induced Th2 cytokine expression[3,7]. We therefore examined Th2- and Th1-associated cytokine mRNA profiles in the liver at 8 and 12 weeks. As expected[8,9], there was a marked elevation in the Th2-associated

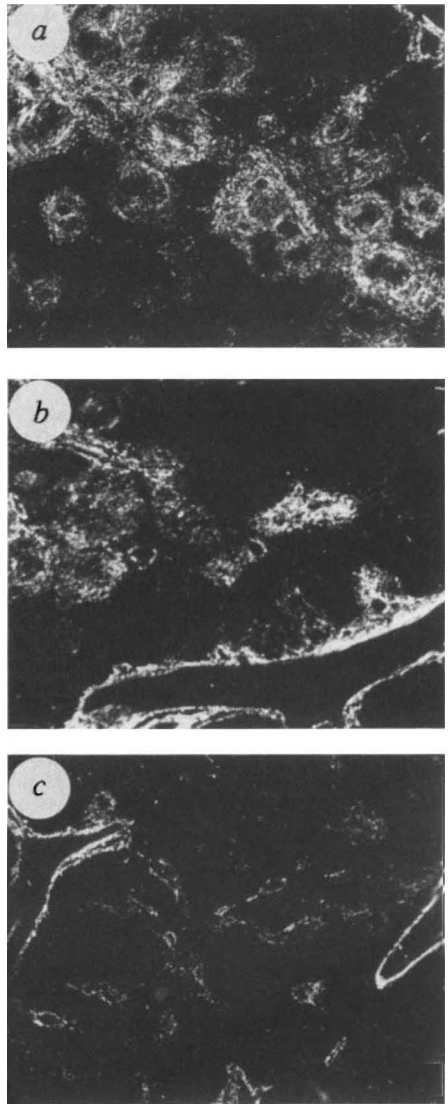

FIG. 1 Hepatic collagen production is reduced in infected mice sensitized with eggs/IL-12. Liver sections were obtained 12 weeks after challenge infection. Unsensitized (*a*), egg/saline-sensitized (*b*), egg/IL-12-sensitized (*c*) and infected mice that contained nearly identical tissue egg burdens were stained with picrosirius red and photographed using polarized light, and the areas shown are representative for each liver. Birefringent areas indicate collagen (magnification, ×34). Liver sections from egg/IL-12-immunized mice showed only slight granuloma and portal tract-associated collagen, in comparison with non-vaccinated animals.